Ultrasonics Sonochemistry 103 (2024) 106781

Contents lists available at ScienceDirect

Ultrasonics Sonochemistry

journal homepage: www.elsevier.com/locate/ultson

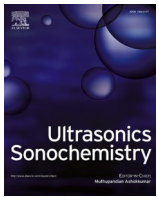

Ultrasonic-assisted activated carbon separation removing bacterial endotoxin from *salvia miltiorrhizae* injection

Cunyu Li [a,b,c,1,*], Shuwan Tang [a,1], Yangyang Xu [a], Fangmei Liu [a], Mingming Li [d], Xinglei Zhi [a], Yun Ma [e,*]

[a] College of Pharmacy, Nanjing University of Chinese Medicine, Nanjing 210023, China
[b] Jiangsu Collaborative Innovation Center of Chinese Medicinal Resources Industrialization, Nanjing 210023, China
[c] National Key Laboratory on Technologies for Chinese Medicine Pharmaceutical Process Control and Intelligent Manufacture, Lianyungang 222067, China
[d] Jiangsu Shenlong Pharmaceutical Co., Ltd, Dongtai 224200, China
[e] The Fourth People's Hospital of Taizhou City, Taizhou 225300, China

ARTICLE INFO

Keywords:
Salvia miltiorrhizae injection
Bacterial endotoxin
Ultrasonic-assisted activated carbon separation
Nanofiltration
Anaphylaxis

ABSTRACT

Ultrasonic-assisted activated carbon separation (UACS) was first employed to improve product quality by regulating adsorption rate and removing bacterial endotoxin from *salvia miltiorrhizae* injection. The adsorption rate was related to three variables: activated carbon dosage, ultrasonic power, and pH. With the increase of activated carbon dosage from 0.05 % to 1.0 %, the adsorption rates of salvianolic acids and bacterial endotoxin increased simultaneously. The adsorption rates at which bacteria endotoxins increased from 52.52 % to 97.16 % were much higher than salvianolic acids. As the ultrasonic power increased from 0 to 700 W, the adsorption rates of salvianolic acids on activated carbon declined to less than 10 %, but bacterial endotoxin increased to more than 87 %. As the pH increased from 2.00 to 8.00, the adsorption rate of salvianolic acid dropped whereas bacterial endotoxin remained relatively stable. On the basis of response surface methodology (RSM), the optimal separation conditions were established to be activated carbon dose of 0.70 %, ultrasonic power of 600 W, and pH of 7.90. The experimental adsorption rates of bacterial endotoxin were 94.15 %, which satisfied the *salvia miltiorrhizae* injection quality criterion. Meanwhile, salvianolic acids' adsorption rates were 1.92 % for tanshinol, 4.05 % for protocatechualdehyde, 2.21 % for rosmarinic acid, and 3.77 % for salvianolic acid B, all of which were much lower than conventional activated carbon adsorption (CACA). Salvianolic acids' adsorption mechanism on activated carbon is dependent on the component's molecular state. Under ideal separation conditions, the molecular states of the four salvianolic acids fall between 1.13 % and 6.60 %. The quality of *salvia miltiorrhizae* injection can be improved while maintaining injection safety by reducing the adsorption rates of salvianolic acids to less than 5 % by the use of ultrasound to accelerate the desorption mass transfer rate on the activated carbon surface. When activated carbon adsorption was used in the process of producing *salvia miltiorrhizae* injection, the pH of the solution was around 5.00, and the proportion of each component's molecular state was tanshinol 7.05 %, protocatechualdehyde 48.93 %, rosmarinic acid 13.79 %, and salvianolic acid B 10.28 %, respectively. The loss of useful components was evident, and the corresponding activated carbon adsorption rate ranged from 20.74 % to 41.05 %. The average variation rate in plasma His and IgE was significant ($P < 0.05$) following injection of 0.01 % activated carbon, however the average variation rate of *salvia miltiorrhizae* injection was dramatically decreased with the use of UACS and CACA ($P > 0.05$). The ultrasonic at a power intensity of 60 W/L and the power density of 1.20 W/cm^2 may resolve the separation contradiction between salvianolic acids and bacterial endotoxin, according to experiments conducted with UACS at different power intensities. According to this study, UACS has a lot of potential applications in the pharmaceutical manufacturing industry and may represent a breakthrough in the field of ultrasonic separation.

* Corresponding authors at: College of Pharmacy, Nanjing University of Chinese Medicine, Nanjing 210023, China (C. Li); The Fourth People's Hospital of Taizhou City, Taizhou 225300, China (Y. Ma).
E-mail addresses: licunyuok@163.com (C. Li), myunok@163.com (Y. Ma).
[1] Cunyu Li and Shuwan Tang contributed equally to this paper.

https://doi.org/10.1016/j.ultsonch.2024.106781
Received 27 December 2023; Received in revised form 19 January 2024; Accepted 22 January 2024
Available online 24 January 2024

1. Introduction

In the fields of medicine, food and water treatment, activated carbon is a common adsorbent that has the dual properties of physical adsorption and chemical adsorption [1–3]. It is frequently used for the removal and decolorization of hazardous compounds. To assure the safety of the clinical usage of the injection, activated carbon is frequently employed as an adsorbent in the manufacturing process to efficiently adsorb pyrogen in the drug solution, increase the safety of the injection, and effectively improve the clarity of the preparation [4–6]. However, as activated carbon lacks the unique property of pyrogen adsorption and instead primarily uses the van der Waals force to adsorb pyrogen and other compounds to carbon chains, it will result in the loss of pharmaceutical components during the adsorption process [7]. There is currently no feasible solution for this problem.

Salvia miltiorrhizae injection is made using various production procedures, including extraction, alcohol precipitation, hydrolysis, activated carbon adsorption, filtration, and other steps. It serves as a typical drug in the clinical treatment of cardiovascular and cerebrovascular diseases like cerebral infarction, hypertension, and coronary heart disease [8,9]. The representative salvianolic acids in *salvia miltiorrhizae* injection that are lost during the pharmaceutical process, particularly in the process of activated carbon adsorption and pyrogen removal, include tanshinol, rosmarinic acid, protocatechualdehyde, and salvianolic acid B [10]. Salvianolic acids are lost as much as 5–70 % throughout the drug preparation process when the activated carbon dose is 0.1–1.0 %. This loss is difficult to prevent. As a result, when pyrogen is removed to assure the safety of injection, the drug's quality is inexorably impacted.

Bacterial endotoxin, the primary cause of clinical pyrogen adverse responses, is lipopolysaccharide on the outer wall of gram-negative bacilli [11,12]. It is simple to be adsorbed by activated carbon due to the lipopolysaccharide structure's surface-like activity, which might encourage the creation of bacterial endotoxin micelles or colloidal particles with molecular weights up to 400,000 Da − 1000,000 Da [13]. Salvianolic acids have a molecular weight of less than 1000 Da and have a van der Waals force that is significantly lower than that of bacterial endotoxin, but they still have a competitive adsorption effect with endotoxin on the surface of activated carbon [14].

Ultrasonic technology is one of the most frequently applied non-thermal processing methods in the green separating industry [15]. The nearby material receives the ultrasonic energy once the surrounding medium begins to vibrate due to the ultrasonic emission. The ultrasonic cavitation effect is caused by microscopic bubbles that form in the liquid nucleation under the influence of ultrasonic activity. Ultrasonic waves exhibit mechanical wave properties, including acceleration, sound pressure, and intensity. The ultrasonic thermal effect is caused by the medium's internal friction heat, which is produced by the medium's powerful high-frequency oscillation [16]. Ultrasound can regulate the adsorption mass transfer efficiency of the adsorbent surface, allowing for the orderly separation of the target components. Copper oxide nanoparticles loaded on activated carbon (CuO-NPs-AC) was used for simultaneous ultrasound-assisted adsorption of brilliant green, auramine O, methylene blue and eosin yellow dyes [17]. Activated carbon composite with HKUST-1 metal organic framework was applied for the simultaneous ultrasound-assisted removal of crystal violet, disulfine blue and quinoline yellow dyes in their ternary solution [18]. By changing the disparities in the adsorption behaviors of salvianolic acid, bacterial endotoxin, and activated carbon with the assistance of ultrasonic cavitation-turbulence effects [19,20], an adjustable adsorption separation method was produced. The technical problem of salvianolic acid and activated carbon adsorption was resolved, and the adsorption capacity of salvianolic acid and activated carbon was decreased without affecting the structure and adsorption properties of bacterial endotoxin. In this experiment, the pH of the solution was modified to change the molecular proportion of salvianolic acids, and ultrasonic power was combined to adjust the adsorption effect of activated carbon.

Response surface methodology (RSM) is a powerful statistical model that has been frequently applied in adsorbent research to optimize process parameters [21,22]. RSM is used to establish a relationship between input items and output responses [23]. In this paper, the influence of solution pH, ultrasonic power, and activated carbon dose on activated carbon adsorption behavior of bacterial endotoxin and salvianolic acids were investigated using RSM [24,25]. Simultaneously, in order to assess the potential problem of activated carbon shedding caused by ultrasonic treatment, a safety evaluation of an animal model for allergic evaluation of injection was performed [26], while ultrasound assisted optimization of activated carbon adsorption parameters was performed, which not only expanded the application scope of ultrasound in the pharmaceutical industry [27], but also provided the research foundation for efficient and standardized injection production.

2. Materials and methods

2.1. Materials

The reference substances of tanshinol (purity ≥ 97.8 %), rosmarinic acid (purity ≥ 98.6 %), protocatechualdehyde (purity ≥ 98.2 %), salvianolic acid B (purity ≥ 96.2 %) were purchased from the National Institute for the Control of Pharmaceutical and Biological Products (Beijing, China). *Salvia miltiorrhizae* injection obtained from Jiangsu Shenlong Pharmaceutical Co., Ltd. (Yancheng, China). Bacterial endotoxin standard substance (Lot No. 150601–201783, 80 EU/Amp) was bought from the National Institute for the Control of Pharmaceutical and Biological Products (Beijing, China). Limulus amebocyte lysate (LAL) (Lot No. 17070312, λ = 0.03 EU/mL) and bacterial endotoxin test water (Lot No. 1709130, 50 mL/Amp) were manufactured by Zhanjiang A&C Biological Ltd. (Guangzhou, China). Egg albumin was obtained from Sigma (Missouri, USA). Guinea pig 5-hydroxytryptamine (5-HT) and histamine (HIS) ELISA test kits were purchased from Shanghai Enzyme-linked Biotechnology Co., Ltd. (Shanghai, China). Methanol, acetonitrile and trifluoroacetic acid were all chromatographic grade and purchased from Merck Chemical Technology Co. Ltd. (Shanghai, China). Activated carbon was pharmaceutical grade and purchased from Ruichengkang Medical Technology Co. Ltd. (Xi'an, China). Ultrapure water was prepared by Millipore Direct-Q5 water purification system.

Male guinea pigs weighing 300 ± 50 g were acquired from Qinglongshan Animal Breeding Center in Nanjing, Jiangning District (license number SYXK 2017–0011). Animals were fed at 22 ℃ and 55 % ±5% relative humidity in the animal breeding center of Nanjing University of Chinese Medicine. The Nanjing University of Chinese Medicine's institutional ethical council authorized this anaphylactic reaction study.

2.2. Conventional activated carbon adsorption (CACA)

After pharmaceutical processes such as extraction, concentration, and alcohol precipitation, *salvia miltiorrhiza* injection was diluted with water in injection and boiled with activated carbon for 30 min before being filtered. The removal impact of bacterial endotoxin by activated carbon adsorption was thoroughly investigated using the changes in the concentrations of bacterial endotoxin, tanshinol, rosmarinic acid, protocatechualdehyde, and salvianolic acid B before and after adsorption by activated carbon. And the adsorption rate of solutes was calculated by Equation (1).

$$\text{Adsorption rate} = (1 - \frac{M_1}{M_O}) \times 100\% \quad (1)$$

Where M_0 and M_1 were the content of the index components before and after adsorption by activated carbon.

2.3. Ultrasonic-assisted activated carbon separation (UACS)

In accordance with the injection process of *salvia miltiorrhiza*, the solution had been exposed to activated carbon adsorption in the SCQ-9200E ultrasonic apparatus, which purchased from Shanghai Shengyan ultrasonic instrument Co. Ltd. (Shanghai, China). The ultrasonic apparatus consisted of an ultrasonic generator and an ultrasonic transducer, with adjustable ultrasonic power ranging from 100 W to 700 W and an ultrasonic frequency of 40 KHz.

2.4. Anaphylaxis evaluation

The Nanjing University of Chinese Medicine Institutional Review Board gave its approval for this study on anaphylactic reaction. The fifty male guinea pigs were split into four equal groups at random: saline, egg albumin, 0.01 % activated carbon, the CACA and UACS of the *salvia miltiorrhiza* injection. The Chinese Pharmacopoeia 2020 states that egg albumin with sodium chloride injection was used to generate a 5.0 mg/mL egg albumin solution. Guinea pigs used in allergy investigations received subcutaneous injections of 0.2 mL test solutions. The guinea pigs were fed according to regular procedures following their initial injection. The guinea pigs were given a 10 % chloral hydrate anesthesia on the sixteenth day, and 1.0 mL of arterial blood was drawn from the carotid artery using a heparin anticoagulation tube. Following the jugular vein injection of the 0.5 mL test solutions, 1.0 mL of arterial blood was drawn using the same procedure 30 min later. Following a 5-minute centrifugation at 4000 rpm, the guinea pig plasma was separated from anticoagulant tubes and kept at −80 ℃. Utilizing ELISA test kits, the content of IgE and histamine (His) in plasma samples were examined [28]. Furthermore, the animal breeding center of Nanjing University of Chinese Medicine handled the cadavers after all guinea pigs were put to death under anesthesia.

2.5. Calculation of molecular proportion of salvianolic acids

Salvianolic acids were quantitatively calculated based on the previously established quantitative calculation method for the existence state, based on the changes in nanofiltration mass transfer behavior caused by the existence state of components [29], and the correlation analysis was conducted with activated carbon adsorption characteristics, in order to explain the adsorption mechanism of salvianolic acids by activated carbon.

In summary, the equipment for nanofiltration separation was purchased from Nanjing Tuozhu Co. Ltd. and was assembled on a laboratory bench. It included a spiral nanofiltration membrane, a single variable-speed gear pump for pressure and recirculation, a digital pressure gauge for monitoring operating pressure, and the necessary tubings. Following precise weighing, the four extracts of salvianolic acid were ultrasonically dissolved in ultrapure water at concentrations of, respectively, 1.240 mg/mL for salvianolic acid B, 0.210 mg/mL for rosmarinic acid, 0.360 mg/mL for tanshinol, and 0.820 mg/mL for protocatechualdehyde, respectively. To ensure that all four components were 99 % present in their molecular forms, the extract solution's pH was adjusted based on the dissociation constants (*pK*a) of each component (salvianolic acid B 2.77, rosmarinic acid 4.01, protocatechualdehyde 7.56, and tanshinol 3.82).

The solutions of the four salvianolic acids were diluted with ultrapure water 2, 4, and 8 times, respectively. Then, the solutions of the series concentration were separated by nanofiltration, with the transmembrane pressure difference being controlled at 0.6, 0.8, 1.0, 1.2, 1.4, and 1.6 MPa. Solutions both prior to and following nanofiltration, as well as the membrane flux (*Jv*) under series pressure, were gathered. The rejection rate (*R*) is calculated by Equation (2).

$$R = (1 - \frac{C_F}{C_O}) \times 100\% \quad (2)$$

Where C_F and C_O were the concentrations of the index components in the filtrate and original solution, respectively.

According to the nanofiltration solution-diffusion theory [30,31], the membrane flux, rejection rate, and membrane separation layer parameters in the nanofiltration separation process of salvianolic acids were fitted, and the mass transfer coefficient (*k*) was calculated using Equation (3), and the power function relationship between the mass transfer coefficient (*k*) and solute concentration (*C*) was calculated using Equation (4).

$$\ln[(1 - R) \bullet J_V/R] = \ln[DK/\delta] + \frac{J_v}{k} \quad (3)$$

$$k = mC^n \quad (4)$$

Where δ was the membrane thickness (cm), and DK/δ was the membrane's mass transfer performance (cm/s).

Equation (3)'s regression coefficient was greater than 0.90, suggesting a strong link between *k* and *C*. Based on this, a mathematical model for the existence state was created. Before activated carbon adsorption, a series of *salvia miltiorrhiza* solutions were separated by nanofiltration, and the power function equations of *k* and *C* were fitted using the mass transfer coefficient and solute concentration power function equations produced by salvianolic acid monomer. Using the same *k* value, the concentration differences between the salvianolic acid monomer solution and the *salvia miltiorrhiza* solutions were compared, and the relationship between the component transfer rate and existence state was examined in order to understand the mechanism of the activated carbon process.

2.6. Single factor experiment

Adsorption specificity is a problem that makes it challenging to prevent salvianolic acid loss when employing activated carbon adsorption for removing bacterial endotoxin from solution. Bacterial endotoxin adsorption and removal in injection are directly correlated with the amount of activated carbon because the lipopolysaccharide structure of bacterial endotoxin and activated carbon adsorbed each other through van der Waals force. When weighing the adsorption of bacterial endotoxin and salvianolic acid by activated carbon, ultrasonic induced cavitation, turbulence, and other factors will modify the adsorption behavior of the solute and activated carbon [32]. Meanwhile, changing the pH of the solution will affect the existing state of salvianolic acids in solution, impacting the van der Waals force between activated carbon and salvianolic acids. Consequently, the main variables influencing activated carbon adsorption are the dosage of activated carbon, the pH of the solution, and the ultrasonic power.

As the single factor experiment proceeds, adjust one factor at a time while keeping the other two unaltered. The fixed level of variables included an activated carbon dosage of 0.5 %, an ultrasonic power of 300 W and a solution pH of 5.00. The dosage of activated carbon was examined at 0.05 %, 0.1 %, 0.2 %, 0.5 %, 0.8 %, and 1.0 %, respectively, in accordance with the injection's manufacturing requirements. 0 W, 100 W, 200 W, 300 W, 400 W, 500 W, 600 W, 700 W, and 800 W were examined based on the power range of the ultrasonic apparatus. The pH values of the solution were 2.00, 3.00, 4.00, 5.00, 6.00, 7.00 and 8.00, based on the pKa of salvianolic acids [33].

2.7. Experiment design and statistical analysis

To optimize process parameters, pharmaceutical research has made extensive use of RSM, an efficient statistical model [34]. The evaluation indicators for salvianolic acid transfer rate and bacterial endotoxin removal rate were determined through a single factor investigation. There were 17 experimental runs used, with 5 replicates at the center point. Regression analysis was performed using the following quadratic

polynomial model based on the experimental data. Each response's quadratic model appeared as the following:

$$Y = \beta_0 + \sum \beta_i X_i + \sum \beta_{ii} X_i^2 + \sum \beta_{ij} X_i X_j \quad (5)$$

Y represents the response value, β_0 denotes the constant, β_i, β_{ii}, and β_{ij} denote the linear and quadratic regression coefficients, while X_i and X_j are the independent variables. The analysis of variance (ANOVA) was utilized to evaluate the statistical significance of the equation. The P-value was used to assess each coefficient's significance as well as the interactions between each independent variable. Each experiment was carried out three times, and the average result was presented.

2.8. Sample analysis

2.8.1. Bacterial endotoxin

With the use of limulus agent dynamic turbidity, the bacterial endotoxin in the samples was quantitatively identified. For the purpose of examining bacterial endotoxins, the bacterial endotoxin standard substance was diluted with water to get final concentrations of 2, 0.5, 0.125, and 0.03125 EU/mL, respectively. The reaction tube was filled with 0.1 mL of each product and placed in front of 0.1 mL of limulus agent before being placed into the bacterial endotoxin detector for absorbance examination. Negative control was run twice and each concentration was run three times. When the absorbance reached 0.20, the reaction time (T) and bacterial endotoxin concentration (C) were computed as a logarithmic function using the least square approach. The standard curve was Log$T$ = 3.0117–0.3620Log$C$, r = -0.9965.

Each sample solution was diluted with a specific multiple of water. In parallel, the diluent of this multiple was prepared into a solution containing bacterial endotoxin standard 0.5 EU/mL. 0.1 mL of the aforementioned solution was added to the reaction tube along with 0.1 mL of limulus reagent beforehand, mixed with a vortex, and placed inside the bacterial endotoxin quantitative detector for detection. For every concentration, two tubes were used twice. Calculations were made to determine the bacterial endotoxin content and average recovery rate. The bacterial endotoxin content of the sample was determined by measuring the bacterial endotoxin value at a dilution ratio closer to 100 % when the average recovery fell between 50 % and 200 %.

2.8.2. Salvianolic acid

The concentrations of salvianolic acid B, rosmarinic acid, protocatechualdehyde and tanshinol were determined by Agilent 1100 HPLC system equip with a PDA detector and Hanbon ODS-2 C_{18} reverse-phase column (4.6 mm × 250 mm, 5 μm). The binary mobile phase consisted of acetonitrile (A) and 0.1 % phosphoric acid aqueous solution (B) was used for gradient elution (0–8 min, 5–13 % A; 8–14 min, 13–15 % A; 14–17 min, 15–23 % A; 17–22 min, 23–25 % A; 22–27 min, 25–27 % A; 27–30 min, 27–35 % A; 30–34 min, 35–5% A; 34–38 min, 5 % A). In addition, the flow rate was 0.8 mL/min, column temperature was 30 ℃, detection wavelength was 285 nm and injection volume was 10 μL, respectively.

50 % methanol was used to make a mixed reference solution including tanshinol, protocatechualdehyde, rosmarinic acid, and salvianolic acid B. The mass concentrations of the components were 2.66, 2.40, 1.80, and 3.86 mg/mL, respectively. Gradient was used to properly absorb and dilute the mix of reference solution into six mass concentrations. Following the chromatographic conditions mentioned above, the samples were injected and examined. The linear equation was then computed using regression, using the peak area as the ordinate (Y) and the component mass concentration as the abscissa (X). $Y_{\text{tanshinol}} = 5480\ X + 9320$, $r = 0.9993$; $Y_{\text{protocatechualdehyde}} = 34900\ X + 15500$, $r = 0.9996$; $Y_{\text{rosmarinic acid}} = 18650\ X + 8510$, $r = 0.9992$; $Y_{\text{salvianolic acid B}} = 12240\ X + 5920$, $r = 0.9995$. The method's precision, repeatability, and recovery rate met the analysis requirements, and the stability of the tested solution was good within 24 h.

2.8.3. IgE and His

The plasma IgE and His level in guinea pigs was measured using ELISA kit (double antibody one-step sandwich method) which purchased from mlbio Co. Ltd. (Shanghai, China). The sensitization of guinea pigs was evaluated by the variation rate of IgE and His, which calculated by Equation (5). Where C_B and C_A are the concentration of IgE and His in plasma before and after stimulating by samples, respectively.

$$\text{Variation rate}\ (\%) = \frac{C_A - C_B}{C_B} \times 100\% \quad (6)$$

3. Results and discussion

3.1. Single factor test

3.1.1. Activated carbon dosage

A popular pharmaceutical technique is the removal of contaminants from medications via activated carbon adsorption. As demonstrated in Fig. 1a, the adsorption rates of salvianolic acids and bacterial endotoxin rose in tandem with the rise in activated carbon, which went from 0.05 % to 1.0 %. Significantly greater than salvianolic acids were the bacterial endotoxin adsorption rates, which rose from 52.52 % to 97.16 % among them. Activated carbon's van der Waals force is more noticeable due to the bacterial endotoxin's larger molecular weight [35]. The sequence of salvianolic acid adsorption rates was protocatechualdehyde > salvianolic acid B > rosmarinic acid > tanshinol, but the order of molecular weight (salvianolic acid B > rosmarinic acid > protocatechualdehyde > tanshinol) was not followed by the adsorption behavior of activated carbon. The fundamental explanation is because the *salvia miltiorrhizae* injection pH is 5.00. Except for protocatechualdehyde, the other three phenolic acid components all exist in ionic state, so the adsorption rate of protocatechualdehyde is the highest on activated carbon, and the adsorption rule of other phenolic acid components is positively correlated with molecular weight.

3.1.2. Ultrasonic power

The adsorption and exchange efficiency of solute on the surface of activated carbon particles can be accelerated by ultrasonic cavitation and turbulence effects [36,37]. As shown in Fig. 1b, the effect of ultrasonic power on adsorption rate fluctuates. The adsorption rate of bacterial endotoxin is rather steady, but the adsorption rate of salvianolic acids varies substantially. The adsorption rates of salvianolic acids on activated carbon decreased to less than 10 % with an increase in ultrasonic power from 0 to 700 W, whereas the adsorption rates of bacterial endotoxin on activated carbon were all higher than 87 %. This suggests that the adsorption differences between salvianolic acids and bacterial endotoxin on activated carbon may be amplified by the separation mode of ultrasonic-assisted activated carbon adsorption. It offers a workable separation strategy to decrease the loss of active components and increase the safety of *salvia miltiorrhiza* injection. Nevertheless, there are differences in the impact of ultrasonic assist on the adsorption rate of salvianolic acid on activated carbon. The phenomenon of first decreasing and then increasing salvianolic acid adsorption on activated carbon is observed during the process of increasing the ultrasonic power from 0 W to 700 W. Among these, procatechualdehyde is relatively evident, suggesting that when the ultrasonic power is higher than 600 W, the adsorption rate of salvianolic acids on activated carbon decreases and then increases. Salvianolic acids reabsorb onto the surface of the activated carbon. The observed anomalous adsorption behavior could potentially stem from the augmentation of adsorption sites on the activated carbon particle surface, resulting from the partial desorption of bacterial endotoxin during the ultrasonic assisted activated carbon adsorption procedure [38]. This, in turn, facilitated the secondary adsorption of salvianolic acids. The results of ultrasonic assisted activated carbon adsorption for bacterial endotoxin elimination in *salvia miltiorrhiza* injection are consistent with prior investigations because it

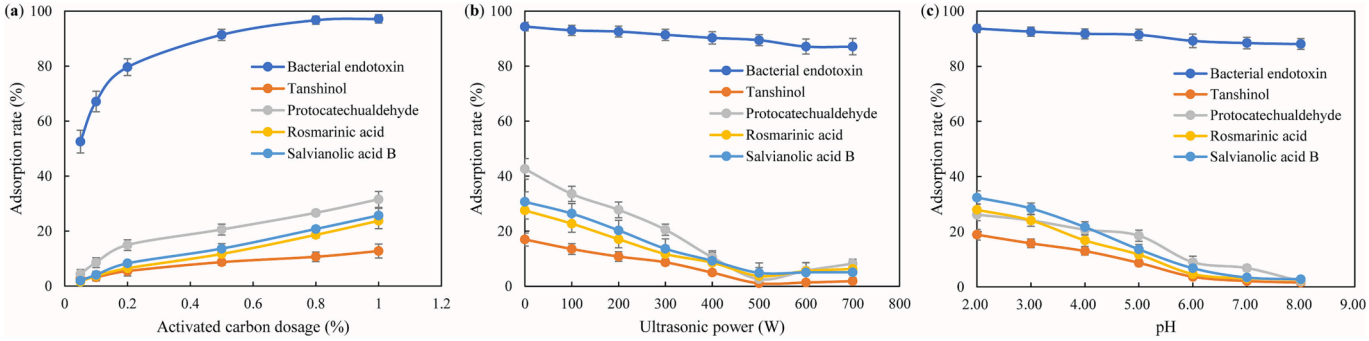

Fig. 1. Effect of factors on the adsorption rate of bacterial endotoxin and salvianolic acids, (a) Activated carbon dosage, (b) Ultrasonic power and (d) pH.

has been demonstrated that ultrasound can destroy the bacterial endotoxin micelle state [13]. The rule of ultrasonic influence on the mass transfer behavior of salvianolic acids by means of activated carbon adsorption is as follows, as shown in Fig. 1b: tanshinol > rosmarinic acid > salvianolic acid B > protocatechualdehyde.

3.1.3. pH

Salvianolic acids' presence in a solution can be controlled by pH. The zero charge (pHzpc) of activated carbon was determined to be 10.70 in order to clarify the adsorption behavior of salvianolic acids on activated carbon. Nevertheless, some of the salvianolic acid B was hydrolyzed when the pH reached 10.7, which had an impact on the adsorption rate computation. After the activated carbon had finished the adsorption experiment, the adsorption rates of four salvianolic acids were less than 1 % after the methanol ultrasonic desorbed the activated carbon. As illustrated in Fig. 1c, there is a transition rule from molecular state to ionic state as pH increases from 2.00 to 8.00, based on the dissociation constants of the four phenolic acids. The adsorption rate of salvianolic acids also exhibit a downward trend because of the weakening of van der Waals force between activated carbon and salvianolic acids. Bacterial endotoxin possesses a lipopolysaccharide structure like to non-ionic surfactants, and the adsorption rate of activated carbon remains generally constant despite variations in solution pH. Salvianolic acids in solution generally reside in an ionic state when the solution pH is 5.00, in contrast to the activated carbon adsorption rate data shown in Fig. 1b and Fig. 1c. The adsorption rates of four phenolic acids fall between 16.96 % and 42.62 % in the absence of ultrasonic treatment. Salvianolic acids are mostly found in molecular form when the pH is raised to 2.00, which increases the van der Waals force between salvianolic acids and activated carbon. Salvianolic acids adsorb at a rate of 18.89 % − 32.37 % when treated with an assisted 300 W ultrasonic power, suggesting that ultrasonic can control the van der Waals force between salvianolic acids and activated carbon [39]. By modifying the solution's pH and the dosage of activated carbon, the separation contradiction between the removal of bacterial endotoxin and the retention of phenolic acid in *salvia miltiorrhiza* injection can be resolved.

Lastly, the primary variables were determined to be the pH, ultrasonic power, and dosage of activated carbon, which varies from 5.00 to 8.00, 400 to 600 W, and 0.2 % to 0.8 %, respectively.

3.2. Statistical analysis and model fitting using RSM

To maximize UACS conditions, 17 experiments (12 factorial and 5 central) were organized and carried out using the Box-Behnken design of RSM. The results are shown in Table 1. The adsorption rates of bacterial endotoxin, tanshinol, protocatechualdehyde, rosmarinic acid and salvianolic acid B were 69.06 % − 97.06 %, 0.21 % − 7.63 %, 0.75 % − 17.19 %, 0.86 % − 13.91 % and 2.03 % − 14.63 %, respectively.

Consequently, the response equation for coded variables was constructed as follows:

$$\text{Bacterial endotoxin}\,(Y_1\%) = 81.42 + 9.69X_1 - 4.36X_2 + 1.29X_3 + 1.21X_1X_2 - 1.28X_1X_3 + 4.73X_2X_3 + 2.56X_1^2 - 0.34X_2^2 + 2.74X_3^2 \quad (7)$$

$$\text{Tanshinol}\,(Y_2\%) = 1.91 + 2.18X_1 - 1.04X_2 - 1.33X_3 + 0.13X_1X_2 - 0.48X_1X_3 + 0.48X_2X_3 + 1.78X_1^2 + 0.48X_2^2 - 0.24X_3^2 \quad (8)$$

Table 1
Response surface design and content results of UACS.

Run	X_1	X_2	X_3	Bacterial endotoxin (%)	Tanshinol (%)	Protocatechualdehyde (%)	Rosmarinic acid (%)	Salvianolic acid B (%)
1	0	−1	1	86.24	1.53	1.67	1.82	3.36
2	0	0	0	82.71	1.66	8.43	2.71	2.85
3	0	0	0	79.78	2.02	9.50	2.04	2.72
4	0	0	0	83.09	1.88	8.57	2.52	2.25
5	−1	−1	0	80.05	3.20	6.73	0.86	5.08
6	0	0	0	81.08	2.05	8.25	2.49	2.68
7	0	0	0	80.44	1.92	8.77	2.62	2.80
8	0	1	−1	73.29	1.80	5.87	5.34	5.02
9	−1	0	−1	75.30	2.25	1.86	3.85	4.06
10	1	0	1	95.58	3.68	5.83	3.98	6.75
11	1	1	0	91.02	5.39	13.67	6.29	8.24
12	0	1	1	86.85	0.42	1.24	1.45	2.03
13	1	−1	0	97.15	7.22	15.76	10.64	12.87
14	−1	1	0	69.06	0.26	0.74	0.85	1.89
15	1	0	−1	97.06	7.63	17.19	13.91	14.63
16	0	−1	−1	91.62	4.82	10.31	9.65	9.97
17	−1	0	1	78.92	0.21	0.75	0.93	2.49

X_1: activated carbon dosage; X_2: ultrasonic power; X_3: pH.

$$\text{Protocatechualdehyde}\,(Y_3\%) = 8.70 + 4.95X_1 - 1.52X_2 - 3.47X_3 + 0.27X_1X_2 - 2.06X_1X_3 + 1.00X_2X_3 + 1.18X_1^2 - 0.96X_2^2 - 2.97X_3^2 \quad (9)$$

$$\text{Rosmarinic acid}\,(Y_4\%) = 2.48 + 3.54X_1 - 1.13X_2 - 3.07X_3 - 1.09X_1X_2 - 1.75X_1X_3 + 0.99X_2X_3 + 1.64X_1^2 + 0.54X_2^2 + 1.55X_3^2 \quad (10)$$

$$\text{Salvianolic acid B}\,(Y_5\%) = 2.66 + 3.62X_1 - 1.76X_2 - 2.38X_3 - 0.36X_1X_2 - 1.58X_1X_3 + 0.91X_2X_3 + 3.12X_1^2 + 1.24X_2^2 + 1.20X_3^2 \quad (11)$$

Using ANOVA, the *F*-value, *P*-value, lack of fit, and *R*-square were used to assess the model's viability and the interactions between the variables. When the *P*-value was less than 0.05, the model term was considered significant. Furthermore, the lack of fit's *P*-value > 0.05 suggested that it was not statistically significant in relation to the pure error. As shown in Table 2, bacterial endotoxin's results were as follows: The model that was employed was of the quadratic type, and its validity was suggested by its *F*-value and *P*-value of 65.34 and < 0.0001, respectively. Here, X_1, X_2, X_3, X_2X_3, X_1^2 and X_3^2 are the significant model terms ($P < 0.05$), whereas the remaining terms were not significant ($P > 0.05$). And The adsorption rate of bacterial endotoxin was affected by variables in the following order: $X_1 > X_2 > X_3$. Moreover, the lack of fit's *P*-value was 0.5742, suggesting that it was not as significant as the pure error. Given that the adjusted R^2 of 0.9731 and the projected R^2 of 0.9202 are in reasonable agreement, it is possible for the model to strongly predict the experimental data.

The adsorption rates of four salvianolic acids were represented in regressions that were statistically significant, as indicated by a *P*-value of less than 0.05 for the model. Furthermore, salvianolic acids' lack of fit *P*-values were higher than 0.5, meaning that they were insignificant in relation to the pure error. In contrast to bacterial endotoxins, the adsorption rate of salvianolic acids was influenced by the following variables: $X_1 > X_3 > X_2$. Every model term had significant effects on the adsorption rates of rosmarinic acid and salvianolic acid B. In the regressions that used protocatechualdehyde, X_2^2 was an insignificant term, while X_3^2 was an insignificant term in the regression that used tanshinol.

The statistical tests for the five models are displayed in Table 3. The adjusted R^2 and the predicted R^2 agreed reasonably well, suggesting that the model was able to strongly predict the experimental values. The C.V. values were 1.61–8.92 %, indicated that the variance of the response variable was relatively small and the experimental results were stable. Additionally, the standard deviations of all the models were less than their means, which accounts for the decreased variability observed in the relationships between the models and the experimental data. All of the models could be used to navigate the design space because the five indexes' adequate precision was greater than 4. In addition, the run numbers 2, 3, 4, 6, and 7 in Table 1 had leverage values of 0.200; the other run numbers had leverage values of 0.750. According to the order of the residual values, bacterial endotoxin, tanshinol, protocatechualdehyde, rosmarinic acid, and salvianolic acid B were −1.64–1.67, −0.25–0.25, −0.59–0.80, −0.44–0.41 and −0.41–0.28. Models and data are reasonable and dependable; residual values are near zero and the difference between the actual and predicted values is minimal. The DFFITS is a criterion for determining the impact measure of an observation in the data. The Influence on fitted value DFFITS of bacterial endotoxin (run numbers 1, 8, 9 and 10), tanshinol (run numbers 9, 10, 12 and 16), protocatechualdehyde (run numbers 1, 8, 13 and 14), rosmarinic acid (run numbers 5, 9, 10, 11, 13 and 14), and salvianolic acid B (run numbers 1, 5, 8, 11, 12 and 16) were the strong response numerical points, respectively. These numerical points suggest

Table 2
Analysis of variance of regression model.

Source	df	Bacterial endotoxin				Tanshinol				Protocatechualdehyde				Rosmarinic acid				Salvianolic acid B			
		Sum of square	Mean square	*F*-value	*P*-value	Sum of Square	Mean Square	*F*-value	*P*-value	Sum of Square	Mean Square	*F*-value	*P*-value	Sum of Square	Mean Square	*F*-value	*P*-value	Sum of Square	Mean Square	*F*-value	*P*-value
Model	9	1081.61	120.18	65.34	<0.0001*	80.04	8.89	165.84	<0.0001*	415.63	46.18	124.07	<0.0001*	231.71	25.75	180.83	<0.0001*	247.03	27.45	327.56	<0.0001*
X_1	1	750.39	750.39	407.98	<0.0001*	40.50	40.50	755.25	<0.0001*	224.40	224.40	602.90	<0.0001*	100.32	100.32	704.63	<0.0001*	104.91	104.91	1251.93	<0.0001*
X_2	1	151.73	151.73	82.49	<0.0001*	9.90	9.90	184.64	<0.0001*	20.96	20.96	56.32	0.0001*	10.22	10.22	71.75	<0.0001*	24.85	24.85	296.57	<0.0001*
X_3	1	13.31	13.31	7.24	0.0311*	14.20	14.20	264.89	<0.0001*	82.82	82.82	222.51	<0.0001*	75.46	75.46	530.00	<0.0001*	45.36	45.36	541.35	<0.0001*
X_1X_2	1	5.90	5.90	3.21	0.1163	0.31	0.31	5.74	0.0477*	3.80	3.80	10.22	0.0151*	4.71	4.71	33.07	0.0007*	0.52	0.52	6.19	0.0418*
X_1X_3	1	6.50	6.50	3.54	0.1021	0.91	0.91	17.01	0.0044*	26.27	26.27	70.57	<0.0001*	12.29	12.29	86.28	<0.0001*	9.95	9.95	118.79	<0.0001*
X_2X_3	1	89.68	89.68	48.76	0.0002*	0.91	0.91	17.01	0.0044*	4.02	4.02	10.80	0.0134*	3.88	3.88	27.26	0.0012*	3.28	3.28	39.10	0.0004*
X_1^2	1	27.54	27.54	14.97	0.0061*	12.25	12.25	228.46	<0.0001*	4.89	4.89	13.15	0.0084*	11.37	11.37	79.85	<0.0001*	41.09	41.09	490.30	<0.0001*
X_2^2	1	0.49	0.49	0.27	0.6203	0.69	0.69	12.93	0.0088*	1.31	1.31	3.51	0.1032	1.23	1.23	8.65	0.0217*	6.44	6.44	76.79	<0.0001*
X_3^2	1	31.55	31.55	17.16	0.0043*	0.12	0.12	2.25	0.1774	47.95	47.95	128.82	<0.0001*	10.09	10.09	70.89	<0.0001*	6.05	6.05	72.21	<0.0001*
Residual	7	12.87	1.84			0.38	0.054			2.61	0.37			1.00	0.14			0.59	0.084		
Lack of fit	3	4.66	1.55	0.76	0.5742**	0.28	0.093	3.93	0.1097**	1.67	0.56	2.37	0.2112**	0.73	0.24	3.63	0.1225**	0.36	0.12	2.10	0.2430**
Pure Error	4	8.22	2.05			0.095	0.024			0.94	0.23			0.27	0.067			0.23	0.057		
Cor Total	16	0.88				80.41				418.23				232.71				247.62			

* means significant, ** means not significant.

Table 3
Statistical tests of compressive strength responses.

Index	Standard deviation	Mean	C.V. %	PRESS	R^2	Adjusted R^2	Predicted R^2	Adequate Precision
Bacterial endotoxin	1.36	84.07	1.61	87.34	0.9882	0.9731	0.9202	26.996
Tanshinol	0.23	2.82	8.21	4.63	0.9953	0.9893	0.9424	41.257
Protocatechualdehyde	0.61	7.36	8.29	28.16	0.9938	0.9858	0.9327	36.390
Rosmarinic acid	0.38	4.23	8.92	12.08	0.9957	0.9902	0.9481	45.698
Salvianolic acid B	0.29	5.28	5.49	6.10	0.9976	0.9946	0.9754	57.231

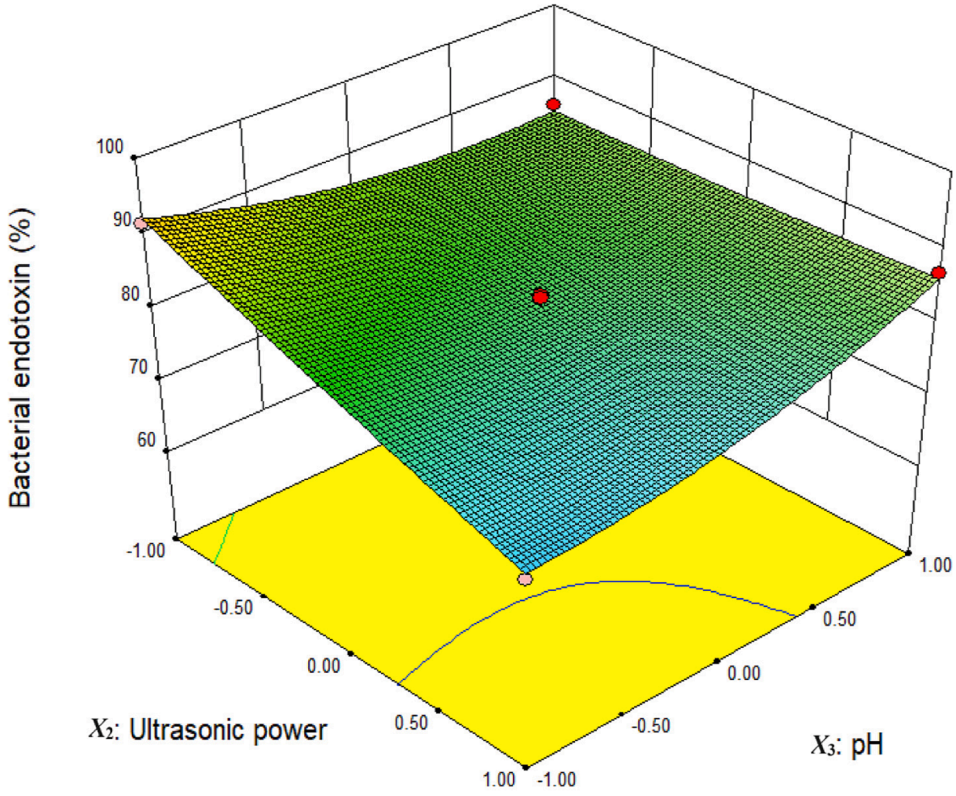

Fig. 2. Interaction effects of ultrasonic power and pH on the adsorption rate of bacterial endotoxin.

a deviation from the predicted data. The mathematical model adjusted R^2 and the predicted R^2 coincided quite well, though, and each group of experiments has been verified three times. As a result, this model can be applied to the experimental research of ultrasonic assisted activated carbon.

The three-dimensional response surface plots were made against two experimental variables while holding the other variable constant in order to assess the effects of all the independent variables and their interactive effects on removing bacterial endotoxin from *salvia miltiorrhizae* injection. As shown in Fig. 2, effect of the interactions between X_2 (ultrasonic power) and X_3 (pH) was obvious, the adsorption rate of bacterial endotoxins exhibited a declining trend with an increase in ultrasonic power, and the influence of pH on the adsorption rate shown diversity. Bacterial endotoxin adsorption first increased and then

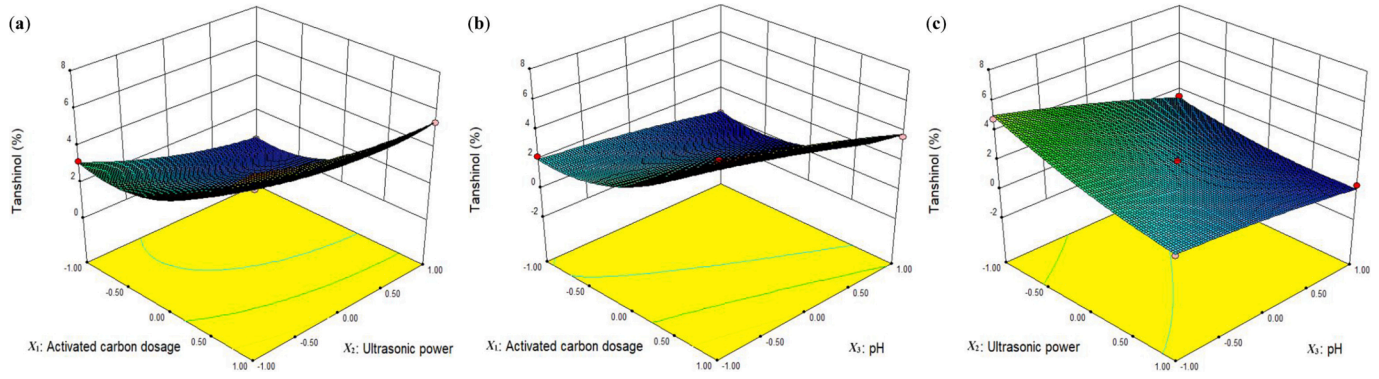

Fig. 3. Interaction effects of (a) Activated carbon dosage and Ultrasonic power, (b) Activated carbon dosage and pH, and (c) Ultrasonic power and pH on the adsorption rate of tanshinol.

reduced with increasing pH within a specific range of ultrasonic power. Presumably, the adsorption rate of bacterial endotoxin rose as a result of the released adsorption site, while the adsorption rate of salvianolic acids reduced as the degree of ionization increased. The bacterial endotoxin's micelles were broken up into smaller ones by ultrasound, which resulted in a decrease in the adsorption rate. Additionally, the alcohol hydroxyl group in the lipopolysaccharide structure of the bacterial endotoxin showed partial ionization with rising pH, further weakening the van der Waals force between the endotoxin and activated carbon.

The degree of X_1 (activated carbon dosage), X_2 (ultrasonic power), and X_3 (pH) influencing the rate of salvianolic acid adsorption is complicated due to the significant interaction among the parameters under investigation. The four salvianolic acids' adsorption rates are positively connected with the X_1 and negatively associated with X_2 and X_3, as shown in Figs. 3–6. To balance the interactions of factors, it is therefore required to determine a point of equilibrium between the adsorption rates of salvianolic acid and bacterial endotoxin. According to Fig. 3, at pH 6.50 and 450 W of ultrasonic power, the adsorption rate first slightly decreased before increasing as the dosage of activated carbon increased from 0.2 % to 0.8 %. This phenomenon became more evident as pH increased, suggesting that ultrasonic accelerated the mass transfer rate of ionic tanshinol on the surface of activated carbon particles when the dosage of activated carbon was low. Tanshinol's adsorption rate steadily dropped as both X_2 and X_3 increased, in line with the adsorption mass transfer theory [40].

Regarding the effect of X_1X_3 and X_2X_3 interaction on the protocatechualdehyde adsorption rate, Fig. 4 illustrates that the adsorption rate first increases and subsequently drops when the ultrasonic power is 500 W and the pH is in the 5.00—8.00 range. The pKa7.56 of protocatechualdehyde indicates that at this point in the solution, the compound underwent a transition from the molecular to the ionic state. The increased adsorption rate during this phase was caused by the presence of three other salvianolic acids in the ionic state, as well as the accelerated desorption of 500 W ultrasound, which released the activated carbon adsorption site and made it easier for the molecular protocatechualdehyde to adsorbed on the surface of the carbon. As pH increased further, protocatechualdehyde's degree of ionization increased as well. Ultrasound was employed to accelerate up the adsorption process, which reduced the adsorption rate.

The interactions between the variables of the rosmarinic acid adsorption rate are displayed in Fig. 5's three-dimensional graphs. Significant interaction was seen between X_1X_2, X_1X_3 and X_2X_3. The adsorption rate of rosmarinic acid decreased as ultrasonic power increased while activated carbon dosage was fixed. Similarly, a pH-induced fluctuation in adsorption rate was also observed. The adsorption rate of salvianolic acid B decreases with increasing ultrasonic power and pH when X_1 is fixed, as illustrated in Fig. 6. Salvianolic acid B's molecular weight is greater than that of the other three salvianolic acids, which results in a greater attraction between it and activated carbon. However, since of its lower adsorption mass transfer efficiency, salvianolic acid B is less sensitive to ultrasonic power. Consequently, in order to achieve a low adsorption rate, a larger ultrasonic power must be applied.

The desirability function was applied to figure out the optimal conditions of UACS. It was discovered that the model's desirability value was 0.996 when the pH was 7.92, the ultrasonic power was 598.34 W, and the activated carbon dose was 0.67 %. Target adsorption rates under ideal conditions were, in order, 92.00 %, 2.00 %, 4.00 %, 2.30 %, and 3.85 % for bacterial endotoxin, tanshinol, protocatechualdehyde, rosmarinic acid, and salvianolic acid B. Verification experiments were carried out under optimal conditions to test the accuracy of the response model: activated carbon dose of 0.70 %, ultrasonic power of 600 W, and pH of 7.90. The experimental adsorption rates of bacterial endotoxin were 94.15 ± 1.01 %, while the adsorption rates of salvianolic acids were as follows: 1.92 ± 0.22 % for tanshinol, 4.05 ± 0.48 % for protocatechualdehyde, 2.21 ± 0.40 % for rosmarinic acid, and 3.77 ± 0.55 % for salvianolic acid B. The application of ultrasonic cavitation effect and turbulence effect resulted in an improvement in the mass transfer efficiency of solute adsorption on activated carbon surface [41]. Additionally, the intermolecular force between activated carbon and salvianolic acids was decreased without impacting the adsorption of bacterial endotoxin, and the desorption efficiency from the surface of activated carbon particles to solution was accelerated. The precision and dependability of RSM in identifying the ideal UACS procedure for eliminating bacterial endotoxin from *salvia miltiorrhiza* injection was validated by the resemblance between the predicted and experimental values.

3.3. Comparison of UACS with CACA

The adsorption rate of bacterial endotoxin was chosen as an index based on RSM's optimal conditions. The experimental adsorption rate with UACS was 94.15 %, which was close to the 97.58 % obtained with CACA, but the experimental adsorption rates of salvianolic acids with UACS were 1.92 % −4.05 %, which was much lower than the 20.74 % − 41.05 % obtained with CACA (Table 4). Salvianolic acids and bacterial endotoxin both showed declining adsorption rates as the amount of activated carbon was reduced. Nonetheless, it was challenging to resolve the conflict between salvianolic acids and bacterial endotoxin regarding activated carbon separation. Due to the bacterial endotoxin's 31.50 % adsorption rate and the salvianolic acid's less than 5 % adsorption rate while using 0.025 % activated carbon, *salvia miltiorrhiza* injection was unable to meet product quality and safety standards [42].

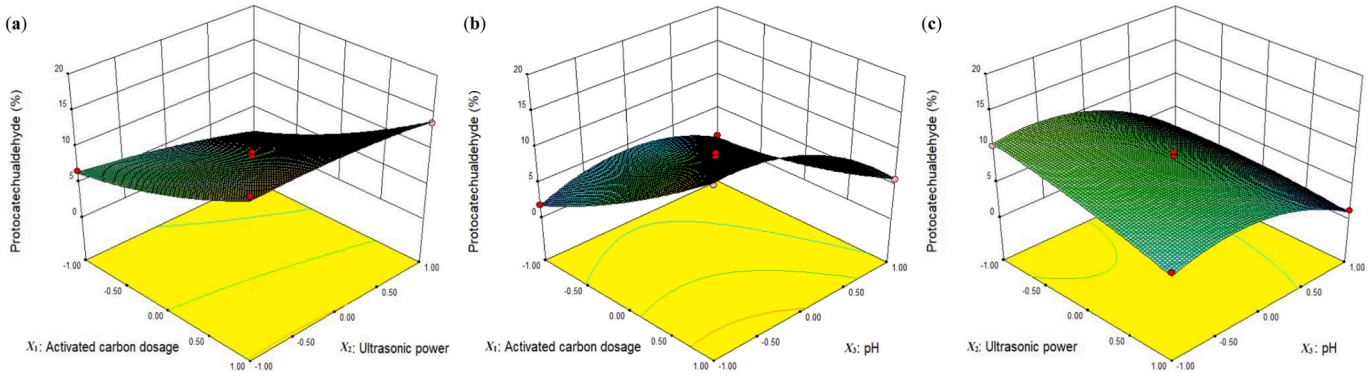

Fig. 4. Interaction effects of (a) Activated carbon dosage and Ultrasonic power, (b) Activated carbon dosage and pH, and (c) Ultrasonic power and pH on the adsorption rate of protocatechualdehyde.

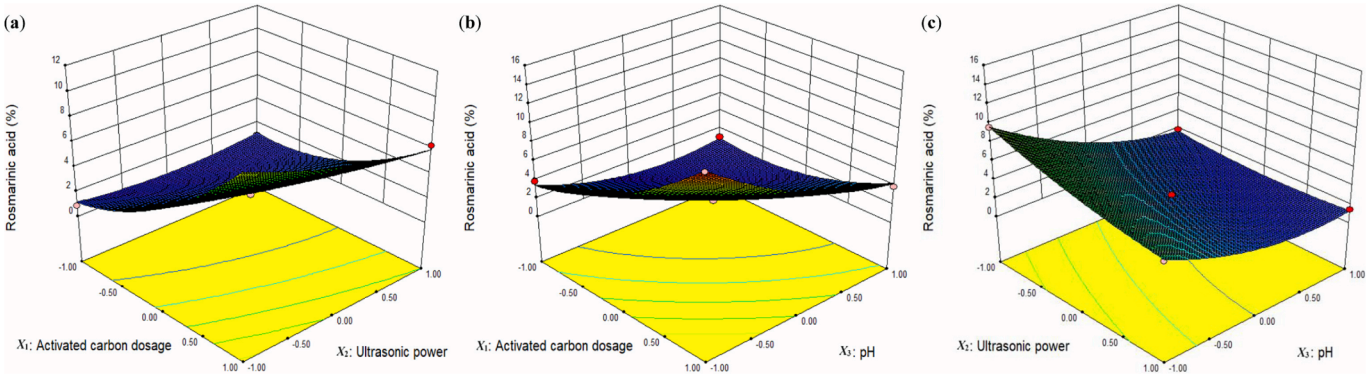

Fig. 5. Interaction effects of (a) Activated carbon dosage and Ultrasonic power, (b) Activated carbon dosage and pH, and (c) Ultrasonic power and pH on the adsorption rate of rosmarinic acid.

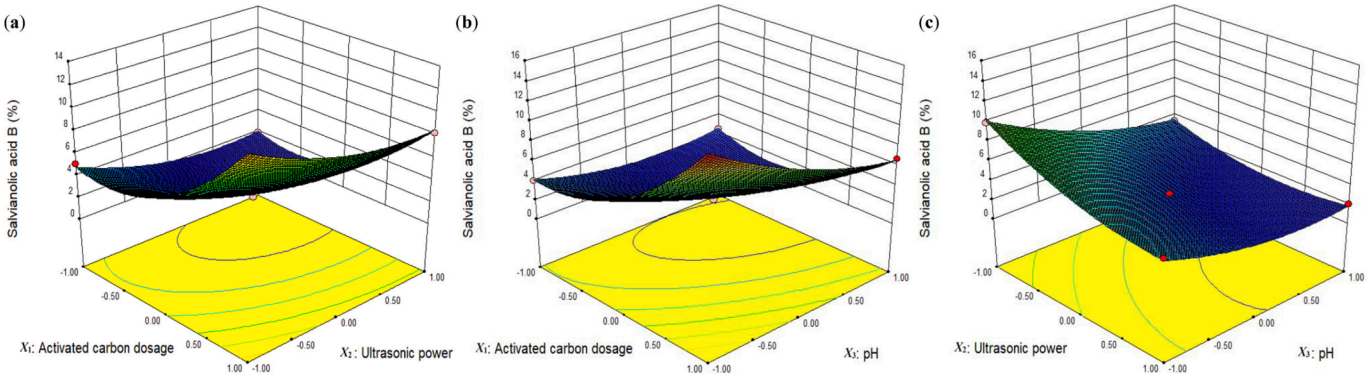

Fig. 6. Interaction effects of (a) Activated carbon dosage and Ultrasonic power, (b) Activated carbon dosage and pH, and (c) Ultrasonic power and pH on the adsorption rate of salvianolic acid B.

Table 4
The adsorption rates (%) of active carbon dosage using CACA.

Active carbon dosage (%)	Bacterial endotoxin	Tanshinol	Protocatechualdehyde	Rosmarinic acid	Salvianolic acid B
0.025	31.50 ± 2.10	1.25 ± 0.40	4.60 ± 0.78	1.73 ± 0.28	2.66 ± 0.61
0.05	54.68 ± 3.67	3.55 ± 0.55	9.52 ± 0.96	4.08 ± 0.53	4.37 ± 0.73
0.1	68.17 ± 3.16	5.40 ± 0.82	14.67 ± 1.61	6.94 ± 1.31	8.58 ± 0.77
0.2	81.39 ± 2.59	7.02 ± 0.95	19.97 ± 2.83	7.70 ± 1.28	10.57 ± 1.10
0.5	92.54 ± 2.03	9.91 ± 1.08	25.04 ± 1.99	13.82 ± 1.70	15.25 ± 1.08
0.7	95.58 ± 1.50	20.74 ± 1.54	41.05 ± 2.55	24.06 ± 3.57	29.72 ± 2.57
1.0	98.42 ± 1.02	31.79 ± 1.77	67.85 ± 2.90	38.29 ± 2.74	45.34 ± 3.62

3.4. Correlation between molecular state and adsorption rate

The correlation equation is as follows, obtained via power function fitting of the concentration of salvianolic acids (C) and the nanofiltration mass transfer coefficient (k): Tanshinol $k = 10.5090C^{0.1095}$, $R^2 = 0.9982$; Protocatechualdehyde $k = 8.9985C^{0.2061}$, $R^2 = 0.9912$; Rosmarinic acid $k = 29.5700C^{0.1676}$, $R^2 = 0.9923$; Salvianolic acid B $k = 12.3990C^{0.1427}$, $R^2 = 0.9923$. Additionally, as shown in Fig. 7, a correlation analysis was conducted with the activated carbon adsorption rate (A) and the molecular proportion (M) of salvianolic acids were determined using the above-mentioned power function equations as the pH rose from 2.00 to 8.00. As the pH of the solution reduced from 8.00 to 2.00, the molecular proportions of the four salvianolic acids increased, and the molecular proportion had a logarithmic association with the adsorption rate of activated carbon. When activated carbon adsorption was used in the process of producing *salvia miltiorrhizae* injection, the pH of the solution was around 5.00, and the proportion of each component's molecular state was tanshinol 7.05 %, protocatechualdehyde 48.93 %, rosmarinic acid 13.79 %, and salvianolic acid B 10.28 %, respectively. The loss of useful components was evident, and the corresponding activated carbon adsorption rate ranged from 20.74 % to 41.05 %. The pH of the solution was adjusted to 7.90 in accordance with the parameters of the UACS, and the component's molecular proportions were as follows: salvianolic acid B1.13 %, rosmarinic acid 2.62 %, tanshinol 3.51 %, and protocatechualdehyde 6.60 %. Even when employing the conventional activated carbon adsorption method, the loss rate of salvianolic acid B was still more than 15 %. The technical difficulties with the *salvia miltiorrhizae* injection manufacturing process was resolved when ultrasound accelerated up the solute's desorption rate on the surface of activated carbon. Bacterial endotoxins were removed at a rate that exceeded 94 %, and the rate of salvianolic acid loss was kept under control at less than 5 %.

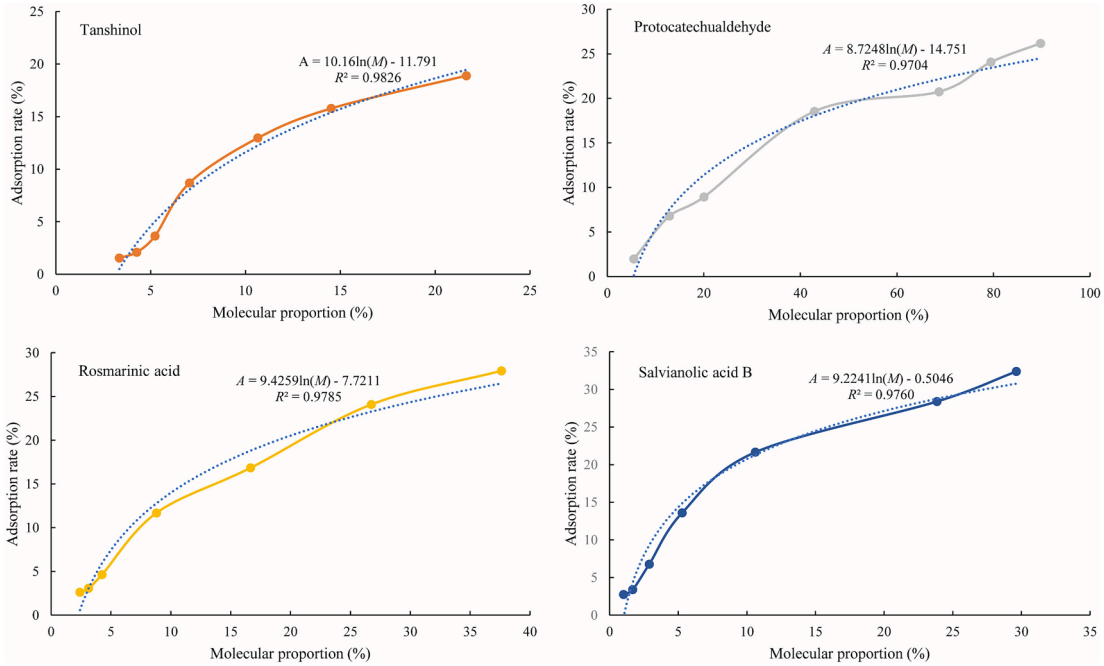

Fig. 7. The correlation between activated carbon adsorption rate and the molecular proportion of salvianolic acids.

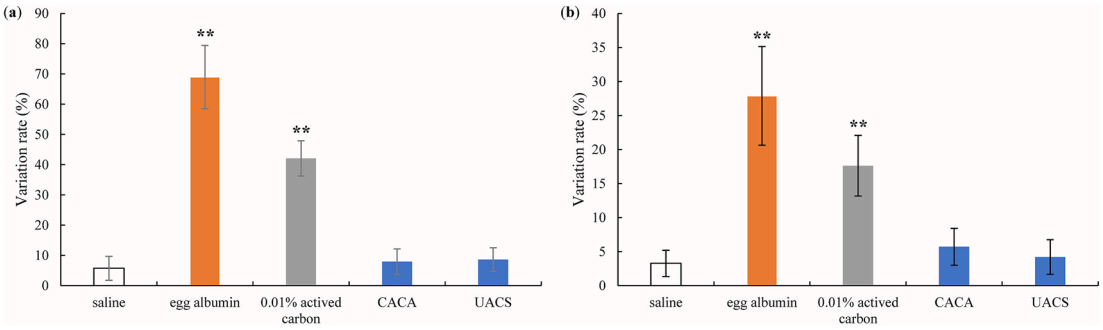

Fig. 8. The variation rate of IgE (a) and His (b) in different group Mean ± SD, $^{**}P < 0.01$ versus saline.

3.5. Anaphylaxis of salvia miltiorrhizae injection

In the *salvia miltiorrhiza* injection manufacturing process, activated carbon serves as a bacterial endotoxins' adsorbent. The ultrasonic treatment increases the frequency of contact between the solute and activated carbon while also modifying their stability, when activated carbon nanoparticles enter *salvia miltiorrhiza* injection perhaps leading to allergic reactions. As shown in Fig. 8, one-way ANOVA was used to assess the sensitization based on the variation rate of IgE and His. IgE and His produced comparable results, in the positive drug group (egg albumin), the average variation rates of IgE and His were 68.96 % and 27.89 %, respectively, and these were significantly greater than in the negative drug group (saline) ($P < 0.05$). The average variation rate in plasma His and IgE was significant ($P < 0.05$) following injection of 0.01 % activated carbon, however the average variation rate of *salvia miltiorrhizae* injection was dramatically decreased with the use of UACS and CACA ($P > 0.05$). The application of ultrasonic-assisted activated carbon has the potential to remove bacterial endotoxin from *salvia miltiorrhizae* injection while having no discernible effect on the components of salvianolic acids and posing no risk of allergic reactions or other potential hazards [43].

4. Conclusion

In this study, an efficient and green UACS method was established to remove bacterial endotoxin from *salvia miltiorrhizae* injection. The obtained second-order polynomial model could fully reflect the influence of independent variables on the response. Since the adsorption behavior of activated carbon is dependent on van der Waals force for non-specific adsorption, it is challenging to prevent the loss of salvianolic acids during the removal of bacterial endotoxins, and the adsorption rate can be affected by activated carbon, ultrasound and pH. As pH rises, the percentage of salvianolic acid molecular states falls. salvianolic acids loss are decreased by the acceleration of desorption efficiency on the activated carbon surface due to the combined effects of ultrasonic cavitation and turbulence. However, there were differences in the effects of pH and ultrasound on salvianolic acids and bacterial endotoxin. By modifying the factor levels, the variations offered a workable strategy for removing the bacterial endotoxin from the *salvia miltiorrhizae* injection.

The RSM approach yielded the following optimal UACS conditions: a pH of 7.90, an activated carbon dosage of 0.70 %, and an ultrasonic power of 600 W. The conflict about the separation of salvianolic acids and bacterial endotoxins has been resolved by UACS as opposed to CACA. UACS can increase the effectiveness of activated carbon's

adsorption and separation while having little effect on injection safety or efficiency.

CRediT authorship contribution statement

Cunyu Li: Writing – review & editing, Project administration, Methodology. **Shuwan Tang:** Writing – original draft, Methodology. **Yangyang Xu:** Writing – original draft, Methodology. **Fangmei Liu:** Writing – review & editing. **Mingming Li:** Supervision, Funding acquisition. **Xinglei Zhi:** Project administration. **Yun Ma:** Writing – review & editing, Methodology.

Declaration of competing interest

The authors declare that they have no known competing financial interests or personal relationships that could have appeared to influence the work reported in this paper.

Acknowledgements

This work was supported by National Natural Science Foundation of China (Grant Nos. 82274106 and 82074006), Natural Science Foundation of Jiangsu Province (Grant No. BK20211303), and Jiangsu Graduate Research and Practice Innovation Project (Grant No. KYCX23_2047).

References

[1] S. Mokhtaryan, A. Khodabakhshi, R. Sadeghi, H. Nourmoradi, K. Shakeri, S. Hemati, F. Mohammadi-Moghadam, New activated carbon derived from Gundelia tournefortii seeds for effective removal of acetaminophen from aqueous solutions: Adsorption performance, Arab. J. Chem. 16 (2023) 105253.
[2] A.A. Tahmasebi, A.S. Beni, A. Azhdarpoor, Z. Moeini, The application of granular and biological activated carbon columns in removal of organochlorine and organophosphorus pesticides in a water treatment plant, J. Water Process Eng. 56 (2023) 104383.
[3] S.P. Selvam, S. Cho, Phosphate-driven H_2O_2 decomposition on DNA-bound bio-inspired activated carbon-based sensing platform for biological and food samples, Food Chem. 421 (2023) 136234.
[4] N.S. Sheraba, A. Hesham, M. Fawzy, E. Diab, M.E. Basuony, A.S. Yassin, H. H. Zedan, M. Abu-Elghait, Advanced approaches for endotoxin detection and removal from snake antivenoms, Toxicon. 222 (2023) 107003.
[5] L. Xu, M. Canales, Q. Zhou, K. Karu, X. Zhou, J. Su, L.C. Campos, L. Ciric, Antibiotic resistance genes and the association with bacterial community in biofilms occurring during the drinking water granular activated carbon (GAC) sandwich biofiltration, J. Hazard. Mater. 460 (2023) 132511.
[6] T.M. Hoogstad, L. Kiewidt, T. van Haasterecht, J.H. Bitter, Size selectivity in adsorption of polydisperse starches on activated carbon, Carbohyd. Polym. 309 (2023) 120705.
[7] N. Malesic-Eleftheriadou, E.V. Liakos, E. Evgenidou, G.Z. Kyzas, D.N. Bikiaris, D. A. Lambropoulou, Low-cost agricultural wastes (orange peels) for the synthesis and characterization of activated carbon biosorbents in the removal of pharmaceuticals in multi-component mixtures from aqueous matrices, J. Mol. Liq. 368 (2022) 120795.
[8] Z. You, Y. Xin, Y. Liu, B. Han, L. Zhang, Y. Chen, Y. Chen, L. Gu, H. Gao, Y. Xuan, Protective effect of Salvia Miltiorrhizae injection on N(G)-nitro-d-arginine induced nitric oxide deficient and oxidative damage in rat kidney, Exp. Toxicol. Pathol. 64 (2012) 453–458.
[9] C. Su, Q. Ming, K. Rahman, T. Han, L. Qin, *Salvia miltiorrhiza*: Traditional medicinal uses, chemistry, and pharmacology, Chin. J. Nat. Med. 13 (2015) 163–182.
[10] Y. Li, L. Song, M. Liu, Z. Hu, Z. Wang, Advancement in analysis of Salviae miltiorrhizae Radix et Rhizoma (Danshen), J. Chromatogr. a. 1216 (2009) 1941–1953.
[11] A. Greenhalgh, O. Istas, R.L. Cooper, Bacterial endotoxin lipopolysaccharide enhances synaptic transmission at low-output glutamatergic synapses, Neurosci. Res. 170 (2021) 59–65.
[12] M. Ochiai, A. Yamamoto, S. Naito, J. Maeyama, A. Masumi, I. Hamaguchi, Y. Horiuchi, K. Yamaguchi, Applicability of bacterial endotoxins test to various blood products by the use of endotoxin-specific lysates, Biologicals. 38 (2010) 629–636.
[13] C. Li, C. Zhao, Y. Ma, W. Chen, Y. Zheng, X. Zhi, G. Peng, Optimization of ultrasonic-assisted ultrafiltration process for removing bacterial endotoxin from diammonium glycyrrhizinate using response surface methodology, Ultrason. Sonochem. 68 (2020) 105215.
[14] F.M.O. Medina, M.B. Aguiar, M.E. Parolo, M.J. Avena, Insights of competitive adsorption on activated carbon of binary caffeine and diclofenac solutions, J. Environ. Manage. 278 (2021) 111523.
[15] S. Mosleh, M.R. Rahimi, M. Ghaedi, K. Dashtian, S. Hajati, Sonochemical-assisted synthesis of CuO/Cu_2O/Cu nanoparticles as efficient photocatalyst for simultaneous degradation of pollutant dyes in rotating packed bed reactor: LED illumination and central composite design optimization, Ultrason. Sonochem. 40 (2018) 601–610.
[16] M. Sun, Y. Zhuang, Y. Gu, G. Zhang, X. Fan, Y. Ding, A comprehensive review of the application of ultrasonication in the production and processing of edible mushrooms: Drying, extraction of bioactive compounds, and post-harvest preservation, Ultrason. Sonochem. 102 (2024) 106763.
[17] S. Dashamiri, M. Ghaedi, K. Dashtian, M.R. Rahimi, A. Goudarzi, R. Jannesar, Ultrasonic enhancement of the simultaneous removal of quaternary toxic organic dyes by CuO nanoparticles loaded on activated carbon: Central composite design, kinetic and isotherm study, Ultrason. Sonochem. 31 (2016) 546–557.
[18] F. Nasiri Azad, M. Ghaedi, K. Dashtian, S. Hajati, V. Pezeshkpour, Ultrasonically assisted hydrothermal synthesis of activated carbon–HKUST-1-MOF hybrid for efficient simultaneous ultrasound-assisted removal of ternary organic dyes and antibacterial investigation: Taguchi optimization, Ultrason. Sonochem. 31 (2016) 383–393.
[19] G. Kozmus, J. Zevnik, M. Hočevar, M. Dular, M. Petkovšek, Characterization of cavitation under ultrasonic horn tip – Proposition of an acoustic cavitation parameter, Ultrason. Sonochem. 89 (2022) 106159.
[20] B. Dong, Y. Guo, J. Yang, X. Yang, L. Wang, D. Huang, Turbulence induced shear controllable synthesis of nano $FePO_4$ irregularly-shaped particles in a counter impinging jet flow T-junction reactor assisted by ultrasound irradiation, Ultrason. Sonochem. 99 (2023) 106590.
[21] V. Pezeshkpour, S.A. Khosravani, M. Ghaedi, K. Dashtian, F. Zare, A. Sharifi, R. Jannesar, M. Zoladl, Ultrasound assisted extraction of phenolic acids from broccoli vegetable and using sonochemistry for preparation of MOF-5 nanocubes: Comparative study based on micro-dilution broth and plate count method for synergism antibacterial effect, Ultrason. Sonochem. 40 (2018) 1031–1038.
[22] M. Rashid, D. Mowla, F. Esmaeilzadeh, K. Dashtian, M. Bahmani, Boosted Cr(VI) clean up over magnetically recoverable NiS/γ-Fe2O3/C type-II heterostructure derived from bimetal (Fe/Ni)-organic framework under visible light, J. Clean. Prod. 317 (2021) 128471.
[23] S.A. Hosseinpour, G. Karimipour, M. Ghaedi, K. Dashtian, Use of metal composite MOF-5-Ag_2O-NPs as an adsorbent for the removal of Auramine O dye under ultrasound energy conditions, Appl. Organomet. Chem. 32 (2018) e4007.
[24] N. Parsazadeh, F. Yousefi, M. Ghaedi, K. Dashtian, F. Borousana, Preparation and characterization of monoliths HKUST-1 MOF via straightforward conversion of Cu (OH)2-based monoliths and its application for wastewater treatment: artificial neural network and central composite design modeling, New J. Chem. 42 (2018) 10327–10336.
[25] Y. Sun, J. Lu, J. Li, P. Li, M. Zhao, G. Xia, Optimization of ultrasonic-assisted extraction of polyphenol from Areca nut (Areca catechu L.) seeds using response surface methodology and its effects on osteogenic activity, Ultrason. Sonochem. 98 (2023) 106511.
[26] D. Wang, C. Pan, J. Han, Y. Zhao, S. Liu, C. Li, Y. Yi, Y. Zhang, X. Tang, A. Liang, Involvement of p38 MAPK/cPLA2 and arachidonic acid metabolic pathway in Shengmai injection-induced pseudo-allergic reactions, J. Ethnopharmacol. 309 (2023) 116357.
[27] H. Liao, W. Huang, L. Zhou, L. Fang, Z. Gao, Q. Yin, Ultrasound-assisted continuous crystallization of metastable polymorphic pharmaceutical in a slug-flow tubular crystallizer, Ultrason. Sonochem. 100 (2023) 106627.
[28] D. Tang, C. Wang, Q. Gan, Z. Wang, R. Jiang, Chemical composition-based characterization of the anti-allergic effect of Guominkang Formula on IgE-mediated mast cells activation and passive cutaneous anaphylaxis, Chin. J. Nat. Med. 20 (2022) 925–936.
[29] C. Li, Y. Lin, M. Li, L. Zhang, S. Li, G. Peng, X. Zhi, Alcohol-precipitation mechanism of Danshen Injection based on molecular state quantitative calculation model, Chin. Tradit. Herbal. Drugs. 53 (2022) 6431–6442.
[30] D. Fierro, A. Boschetti-de-Fierro, V. Abetz, The solution-diffusion with imperfections model as a method to understand organic solvent nanofiltration of multicomponent systems, J. Membr. Sci. 413–414 (2012) 91–101.
[31] L. Pérez, I. Escudero, M.J. Arcos-Martínez, J.M. Benito, Application of the solution-diffusion-film model for the transfer of electrolytes and uncharged compounds in a nanofiltration membrane, J. Ind. Eng. Chem. 47 (2017) 368–374.
[32] Y. Wu, J. Mondal, Y. Tao, G.J.O. Martin, M. Ashokkumar, Ultrasound-enhanced adsorption of amino acids from aqueous solution onto macroporous resins for green separation: Mass transfer mechanism and acoustic cavitation properties, Sep. Purif. Technol. 330 (2024) 125368.
[33] J. Su, J. Qian, W. Zeng, Y. Wang, G. Kai, Effective adsorption of salvianolic acids with phenylboronic acid functionalized polyethyleneimine-intercalated montmorillonite, Sep. Purif. Technol. 311 (2023) 123304.
[34] S. Zhang, H. Xie, J. Huang, Q. Chen, X. Li, X. Chen, J. Liang, L. Wang, Ultrasound-assisted extraction of polyphenols from pine needles (Pinus elliottii): Comprehensive insights from RSM optimization, antioxidant activity, UHPLC-Q-Exactive Orbitrap MS/MS analysis and kinetic model, Ultrason. Sonochem. 106742 (2023).
[35] Y. Liu, Y. Lin, B. Cao, K. Wu, L. Wang, Enhancement of polysiloxane/epoxy resin compatibility through an electrostatic and van der Waals potential design strategy, Polym. Test. 117 (2023) 107820.
[36] Y. Zhou, B. Tawiah, L. Wang, Q. Li, Enhancing the affinity and adsorption efficiency of *Glochidion ericarpum* Champ leave extract to cotton for colouristic and functional properties integrating trimethyl chitosan and ultrasonic technique, Ind. Crop. Prod. 186 (2022) 115255.

[37] M. Esfandyari, A.A. Delouei, A. Jalai, Optimization of ultrasonic-excited double-pipe heat exchanger with machine learning and PSO, Int. Commun. Heat. Mass. Transf. 147 (2023) 106985.
[38] Y. Xu, Y. Chen, C. Ma, W. Qiao, J. Wang, L. Ling, Functionalization of activated carbon fiber mat with bimetallic active sites for NH_3 and H_2S adsorption at room temperature, Sep. Purif. Technol. 303 (2022) 122335.
[39] Z. Pan, Y. Bo, Y. Liang, B. Lu, J. Zhan, J. Zhang, J. Zhang, Intermolecular interactions in natural deep eutectic solvents and their effects on the ultrasound-assisted extraction of artemisinin from *Artemisia annua*, J. Mol. Liq. 326 (2021) 115283.
[40] A. Sánchez-Díaz, A.I. Zárate-Guzmán, E. Bailón-García, N. Medellín-Castillo, E. Padilla-Ortega, A. Aguilar-Aguilar, R. Flores-Ramírez, R. Ocampo-Pérez, Elucidating the low-frequency ultrasound effect on mass transfer resistances during phenol adsorption over microporous materials, J. Water. Process. Eng. 47 (2022) 102790.
[41] Y. Tao, Y. Wu, Y. Han, F. Chemat, D. Li, P.L. Show, Insight into mass transfer during ultrasound-enhanced adsorption/desorption of blueberry anthocyanins on macroporous resins by numerical simulation considering ultrasonic influence on resin properties, Chem. Eng. J. 380 (2020) 122530.
[42] Y. Chang, W. Zhang, Y. Xie, X. Xu, R. Sun, Z. Wang, R. Yan, Postmarketing safety evaluation: depside salt injection made from Danshen (Radix Salviae Miltiorrhizae), J. Tradit. Chin. Med. 34 (2014) 749–753.
[43] C. Li, Y. Ma, L. Ma, X. Zhi, G. Peng, Improving the clarity and sensitization of polysorbate 80 by ultrasonic-assisted ultrafiltration technology, Eur. J. Pharm. Sci. 159 (2021) 105719.